Article

Photocatalytic Degradation of Sulfolane Using a LED-Based Photocatalytic Treatment System

Sripriya Dharwadkar, Linlong Yu * and Gopal Achari

Department of Civil Engineering, University of Calgary, 2500 University Dr. NW, Calgary, AB T2N 1N4, Canada; sdharwad@ucalgary.ca (S.D.); gachari@ucalgary.ca (G.A.)
* Correspondence: linyu@ucalgary.ca; Tel.:+1-403-220-5014

Abstract: Sulfolane is an emerging industrial pollutant detected in the environments near many oil and gas plants in North America. So far, numerous advanced oxidation processes have been investigated to treat sulfolane in aqueous media. However, there is only a few papers that discuss the degradation of sulfolane using photocatalysis. In this study, photocatalytic degradation of sulfolane using titanium dioxide (TiO_2) and reduced graphene oxide TiO_2 composite (RGO-TiO_2) in a light-emitting diode (LED) photoreactor was investigated. The impact of different waters (ultrapure water, tap water, and groundwater) and type of irradiation (UVA-LED and mercury lamp) on photocatalytic degradation of sulfolane were also studied. In addition, a reusability test was conducted for the photocatalyst to examine the degradation of sulfolane in three consecutive cycles with new batches of sulfolane-contaminated water. The results show that LED-based photocatalysis was effective in degrading sulfolane in waters even after three photocatalytic cycles. UVA-LEDs displayed more efficient use of photon energy when compared with the mercury lamps as they have a narrow emission spectrum coinciding with the absorption of TiO_2. The combination of UVA-LED and TiO_2 yielded better performance than UVA-LED and RGO-TiO_2 for the degradation of sulfolane. Much lower sulfolane degradation rates were observed in tap water and groundwater than ultrapure water.

Keywords: sulfolane; diisopropanolamine; photocatalysis; UVA; LED; reduced graphene oxide

1. Introduction

Sulfolane (tetrahydrothiophene-1,1-dioxide), an organosulfur compound, is commonly used as an industrial solvent in the Sulfinol process to remove impurities from sour natural gas [1]. It is also used as a solvent for extraction, extractive distillation, production of polymers, and other electrical applications [2]. Sulfolane is highly soluble in water, with a solubility of 1266 g/L at 20 °C [2]. It does not easily volatilize from water or soil, as shown by its low vapor pressure (0.01 kPa at 20 °C) and low Henry's constant (8.9×10^{-10} atm·m^{-3}·mol^{-1}). According to adsorption studies conducted on aquifer sediments collected in western Canada, sulfolane displays a low average soil-water partition coefficient (kd) of 0.08 L/kg and an organic carbon partition coefficient (KOC) of log 0.07 [3]. Extensive industrial application of sulfolane in gas processing has led to increasing accounts of accidental release into the environment. Sulfolane contamination varying from a few ppb to hundreds of ppm was reported in groundwater and soil near gas processing plants as well as chemical manufacturing facilities, with the most prevalent cause being the mishandling and improper disposal of process waste and spent sulfolane catalysts [4]. Sulfolane is highly mobile in subsurface waters, eventually reaching ecological and human receptors far from the contaminated source [2]. Toxicity studies conducted on various test species have shown the potential adverse effects sulfolane exposure may have on ecological receptors. Acute doses of sulfolane have been shown to inhibit thermoregulatory response of metabolic rate in rats [5]. Sub-acute levels of sulfolane caused convulsions, inflamed lungs, and death in most test species [6]. A recent study involving zebrafish embryos

showed significant developmental impairment after exposure to sulfolane levels found in contaminated environment [7]. As a result, sulfolane has emerged as a contaminant of public concern. In Canada, the Canadian Council of Ministers of the Environment (CCME) established the tolerable daily intake (TDI) for human receptors as 0.0091 mg/kg-bw/day and the guideline for groundwater sulfolane levels as 0.09 mg/L [2].

Sulfolane is considered a persistent contaminant that can be challenging to treat due to its chemical properties. Natural attenuation of sulfolane in oxygen-deficient conditions, such as subsurface aquifers, is insignificant [8]. However, studies conducted on aquifer sediments from sulfolane-contaminated sites found that sulfolane can be biodegraded aerobically by indigenous microbes in nutrient-rich conditions [9,10]. Treatment of sulfolane using biological activated carbon has also been demonstrated on a pilot scale [11]. Although biological treatment has widespread application for water treatment purposes, management and maintenance of a microbial population can be a serious limitation. Studies investigating sulfolane degradation using advanced oxidation processes (AOP) have also emerged more recently. Yu et al. [12] found that ultraviolet (UV) irradiation in combination with either peroxide (H_2O_2) or ozone (O_3), alone, or H_2O_2 and O_3, together, all effectively degraded sulfolane in an aqueous medium. In an extension to this study, Mehrabani-Zeinabad et al. [13] achieved similar results using $UVC/O_3/H_2O_2$ combination, finding that more than 99% of sulfolane could be mineralized to carbon dioxide (CO_2), water, and sulfate ions (SO_4^{2-}). Izadifard et al. [14] demonstrated that activated persulfate with UVC and UVC/O_3 successfully degraded sulfolane in water. Khan et al. [15] successfully reduced degradation time by using an integrated aerobic biodegradation and UVC/H_2O_2 process to treat sulfolane-contaminated water.

A drawback for the reporting AOPs used for sulfolane treatment is the transportation, management, and costs of hazardous chemical oxidants [16]. Photocatalysis is a type of AOP that uses light energy and a semiconductor catalyst to generate hydroxyl ($\cdot OH$) radicals in the presence of water, which does not require handling of large amounts of hazardous chemical oxidants. Heterogeneous photocatalysis using titanium dioxide (TiO_2) has been widely used as a means to treat organics from water due to its chemical stability, durability, low cost, non-toxic nature, and mild operating requirements [17,18]. When TiO_2 in solution is irradiated by photons with higher energy than its bandgap energy, photogenerated holes and electrons on the surface of TiO_2 react with electron donors and acceptors to generate $\cdot OH$ radicals [19–21]. In recent years, studies have shown that efficacy of TiO_2 photocatalysis can be improved by introducing graphene/reduced graphene oxide (RGO), which is claimed to suppress the recombination of photogenerated electron-hole pairs and narrow the bandgap of the catalysts [22–26]. Graphene-based TiO_2 photocatalyst showed higher photocatalytic degradation of dyes such as methylene blue, rhodamine B, and acid orange II [26].

The objective of this study is to investigate the application of UV-LEDs in the photocatalytic degradation of sulfolane using a commercial TiO_2 powder (P25) and RGO-P25 composite synthesized from the hydrothermal method. LEDs have emerged as a source of irradiation that offer many advantages over mercury lamps, which are conventionally used for photocatalytic applications. LEDs have the ability to emit a narrower band of wavelengths, making them a tunable source of light [27]. They have also been associated with better reactor design owing to longer lifetime and compact size [28]. Apart from being energy efficient, LED lamps offer a non-toxic alternative to mercury UV lamps, which require careful handling and disposal due to their toxic constituents [29]. The application of photocatalysis using TiO_2 in conjunction with LED light sources has been reported for treatment of many organics [30–32]. Dharwadkar et al. [33] reported that photocatalytic degradation of sulfolane in a LED reactor can be enhanced with addition of oxidants/adsorbents. In this study, the performance of a LED reactor in photocatalytic degrading sulfolane was compared to fluorescent (mercury) lamps. Matrix effects as well as the impact of a common co-contaminant, diisopropanolamine (DIPA), on photocatalytic

degradation of sulfolane was examined. Finally, the photocatalytic activity of TiO$_2$ for degradation of sulfolane was evaluated in repeated photocatalytic cycles.

2. Results and Discussion

2.1. Photocatalytic Degradation of Sulfolane Using Different Configurations of TiO$_2$

Degradation of sulfolane was studied using P25 and RGO-P25. It is noted that the dosage of P25 and RGO-P25 were the same. The normalized concentrations of sulfolane over the duration of the 30 min dark and 3 h irradiation experiments are shown in Figure 1a. The dark experiment revealed that the adsorption of sulfolane on P25 and RGO-P25 was weak. RGO-P25 even exhibited a lower capacity on adsorbing sulfolane. RGO-P25 was reported to show a high adsorption for dyes [34], but a low adsorption for Bisphenol A [35]. The sample containing P25 powder degraded over 99% of sulfolane in 3 hours of irradiation. Although RGO-P25 was successful in reducing sulfolane concentration, it only degraded about 47% of the original 50 mg/L of sulfolane in 3 hours of irradiation. The pseudo-first-order degradation rate of sulfolane using P25 powder was 70% faster when compared with RGO-TiO$_2$.
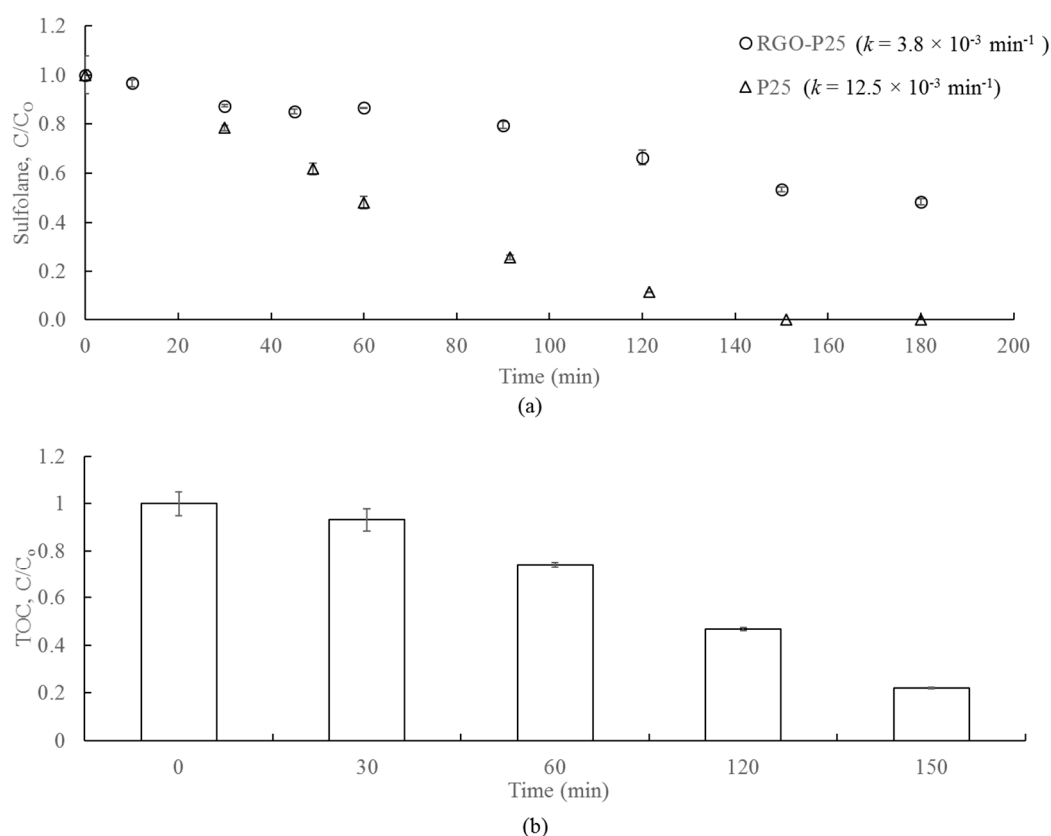
Figure 1. (**a**) Adsorption and photocatalytic degradation of sulfolane using P25 and RGO-P25, (**b**) the change of TOC concentrations during photocatalytic degradation of sulfolane by P25.

The concentration of total organic carbon (TOC) was measured for photocatalytic degradation of sulfolane using P25. The normalized TOC concentrations, at 30 min intervals and for a total of three hours of irradiation time, are shown in Figure 1b. After three hours, TOC was reduced to 22% of the initial concentration, indicating that 78% mineralization of sulfolane was achieved. Degradation of sulfolane during photocatalytic oxidation took place by way of attack by hydroxyl radicals generated through activation of the photocatalyst by photons ($\lambda \approx 365$ nm) emitted by the UVA-LEDs. The pathway for sulfolane degradation by oxidation is not yet well-studied. Yu et al. [12] proposed that the hydroxyl radical may react with sulfolane to produce intermediate radical species by either

the extraction of a hydrogen atom or by reacting with the sulfur atom, triggering the fission of the C-S bonds.

Graphene/carbon-based TiO_2 composites have been reported to display enhanced photocatalytic performance for the degradation of dyes and other compounds when compared with pure TiO_2 photocatalysts [36–40]. Li et al. [34] observed that adsorption of reactive black 5 (RB5) by TiO_2 was increased from less than 5% to more than 50% with the presence of graphene. A faster RB5 degradation rate was also observed with TiO_2-graphene composite. Ruidiaz-Martinez et al. [26] synthesized RGO-TiO_2 composites for ethylparaben degradation and found that the photocatalytic degradation rate was increased from 0.031 to 0.096 min^{-1} when the RGO content in RGO-TiO_2 composite was changed from 0% to 7%. However, Yu et al. [35] found that RGO-TiO_2 composite containing >3% RGO reduced the catalytic degradation of Bisphenol A as the color of the catalyst becomes darker to shield the light.

The enhancement observed in previous works can be attributed to (1) bandgap reduction and (2) the adsorb and shuttle phenomena. The wavelength of light required to achieve activation of the photocatalyst is determined by the bandgap energy (E_g) of the photocatalyst. The bandgap of P25-TiO_2 is in the range of 3.10–3.2 eV, corresponding to the energy of photons with a wavelength of 387–400 nm [41,42]. Studies have shown that graphene-based composites can be used to reduce the bandgap of TiO_2 and extend its photocatalytic application into longer wavelengths [43,44]. Doping with RGO, a graphene derivative, also led to better charge separation, slower recombination, and more efficient production of radical species on the surface of TiO_2 [35]. In the case of the adsorb and shuttle phenomena, a mechanism is proposed to explain the advantage of TiO_2 coated with carbon-based adsorbents based on a two-phase approach. The first phase acts as an adsorbent, adsorbing the substrate, which then transfers it via diffusion to the second phase, the photoactivated site [39]. On the RGO phase, a large number of π–π conjugated double bonds facilitate the adsorption of organic molecules onto the graphene surface [35]. In addition, RGO-TiO_2 were reported to have a larger BET (Brunauer, Emmett, and Teller) surface area than TiO_2 [26,34], which might favor adsorption.

The advantages of RGO-P25 due to the two phenomena, however, were not observed in this study, as (1) the LED light source applied in this study has a maximum emission at 365 nm with narrow emission band. Most of the photons emitted from this light source were already available for photocatalysis with P25. Therefore, the reduction of bandgap energy of photocatalyst did not significantly increase the number of photons contributing to photocatalytic degradation of sulfolane. (2) Our dark adsorption experiments showed that the adsorption of sulfolane on both P25 and RGO-P25 particles are less than <3%. The adsorption of sulfolane on RGO-P25 was too weak to demonstrate the benefit of adsorb-shuttle. A loss of two-dimensional structure of graphene can be caused by aggregation of graphene during the reduction of graphene from graphene oxide and synthesis of RGO-P25 [45,46]. This significantly alters graphene's electrical conductivity, surface area, and optical transparency, potentially blocking active sites on the surface of TiO_2. Reducing the surface area of TiO_2 exposed to irradiation and water molecules also reduces electron hole and hydroxyl radical formation, therefore reducing photocatalytic activity [47]. Furthermore, Akhavan et al. [48] reported a decrease of carbon content in TiO_2-RGO composite by increasing the irradiation time from 4 to 24 h, indicating that a long irradiation might lead to a degradation of RGO by TiO_2 and lower its the catalytic efficiency.

2.2. Effect of Type of Lamp on Photocatalytic Degradation of Sulfolane

In order to study the effect of different sources of irradiation on the photocatalytic oxidation of sulfolane, the performances of UVA and UVC fluorescent mercury lamps were compared with that of UVA-LEDs. The normalized concentrations of sulfolane over varying energy doses from each of the irradiation sources tested are shown in Figure 2. The results show that all irradiation sources used were able to degrade over 99% of sulfolane with less than 600 Joules (J) of photon energy. The bandgap energy of TiO_2 defines that optimal

photocatalytic performance occurs when used with light at wavelengths under 387 nm [49]. The light sources used in this study emit the highest percent of light at wavelengths below this threshold and, as a result, were able to achieve sufficient photoactivation of TiO$_2$ to oxidize sulfolane.
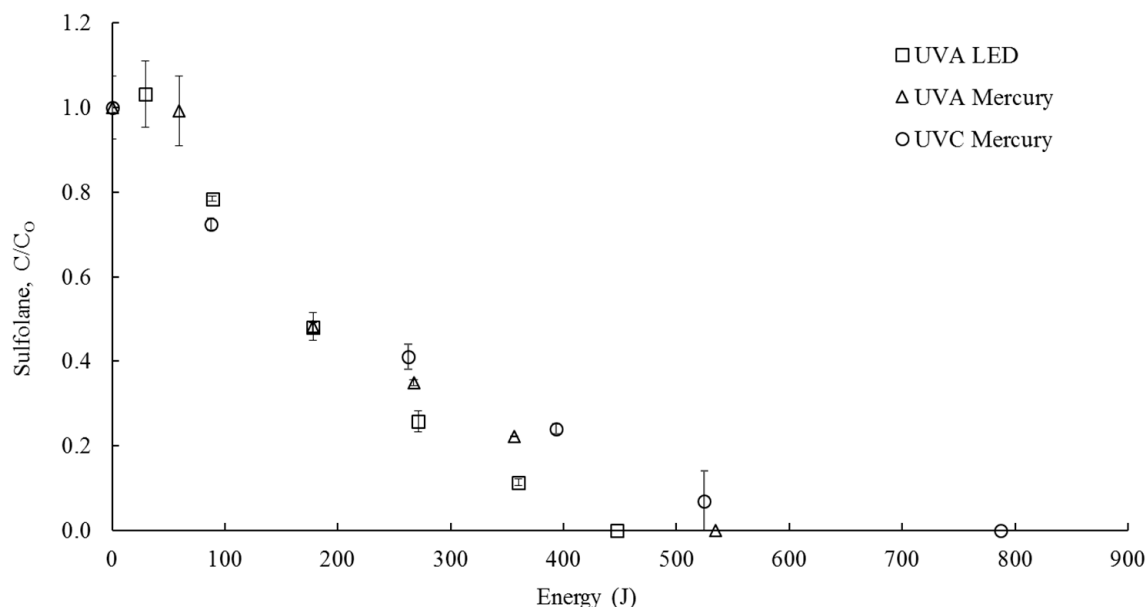
Figure 2. Photocatalytic degradation of sulfolane by 2 g/L of P25 using UVA-LEDs, UVA mercury lamps, and UVC mercury lamps.

To quantitatively compare the three lamps, the photon energy required to achieve one order reduction of sulfolane was calculated for each lamp and summarized in Table 1. It is noted that the photon energy calculated here refers to the energy entering the reaction vessel and not that which is emitted by the lamps. For the UVA-LED reactor, 360 J of photon energy was needed for a one log reduction of sulfolane. UVA mercury and UVC mercury systems required 443 and 496 J of photon energy to remove 90% of sulfolane from solution, which corresponds to 23% and 38% more than UVA-LED, respectively. Yu et al. [30] observed similar results from photocatalytic degradation of a recalcitrant pesticide, 2,4-D. They found that UVA mercury lamps took 26% more photon energy than UVA-LED to obtain a one order reduction in 2,4-D concentration. Two possible theories have been proposed by the author to explain this result. First, UVA-LEDs emitted photons at a narrower range of wavelengths within the required range for photoactivation of TiO$_2$, which led to more efficient photon utilization. Second, UVA-LED, UVA, and UVC mercury lamps have the maximum emissions at 365, 350, and 254 nm, respectively. A shorter wavelength is associated with a higher photon energy requirement to degrade the contaminant.

Table 1. Photon energy consumption in photocatalytic degradation of sulfolane.

Lamp Type	Wavelength (nm)	Intensity (photon/s)	Photon Energy Required to Reach 1-Order Reduction (J)
UVA-LED	353–377	9.06×10^{16}	360
UVA (Mercury)	315–400	1.74×10^{17}	450
UVC (Mercury)	235–280	1.85×10^{17}	487

2.3. Photocatalytic Degradation of Sulfolane in Various Water Matrices

Figure 3 shows the results for sulfolane degradation observed in milli-Q water, groundwater, and tap water. Degradation of sulfolane was observed in all matrices tested, however,

only the milli-Q water spiked with sulfolane reached non-detectable levels of sulfolane in the 3 h of irradiation time, while 29% and 32% of sulfolane was remaining in tap water and groundwater at the end of the reaction time, respectively. Degradation of sulfolane in all matrices followed first-order kinetics, with milli-Q water showing the highest rate of degradation. For all matrices tested, no significant decrease in sulfolane concentration (<3%) was observed during the initial 30 min of dark time.
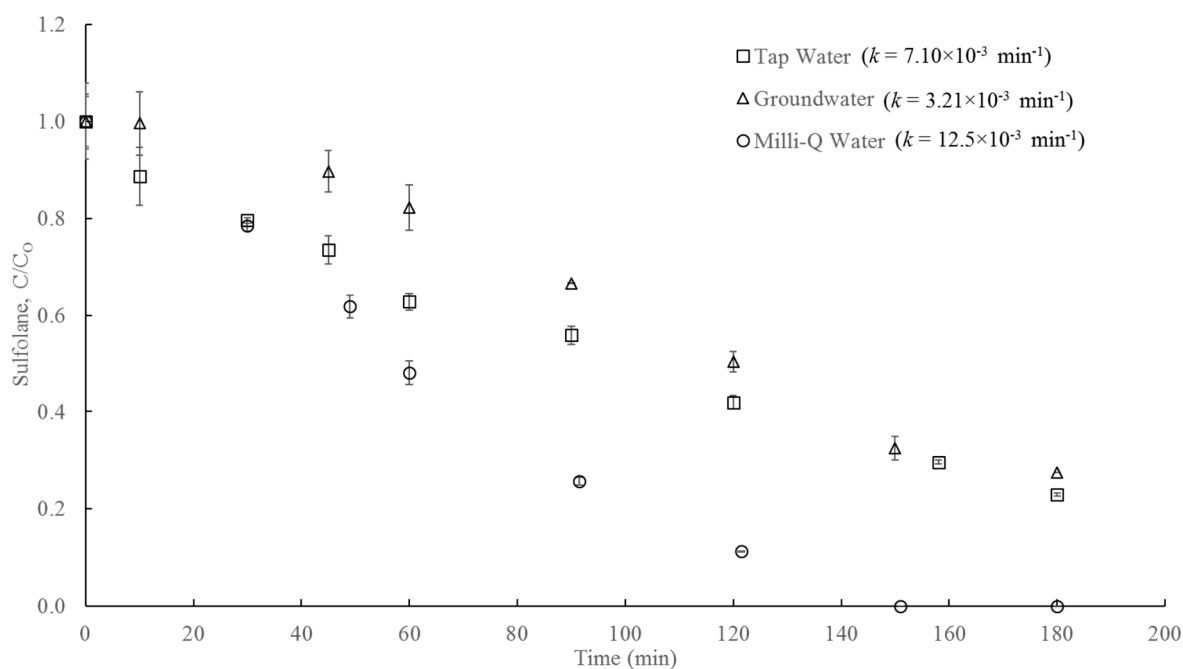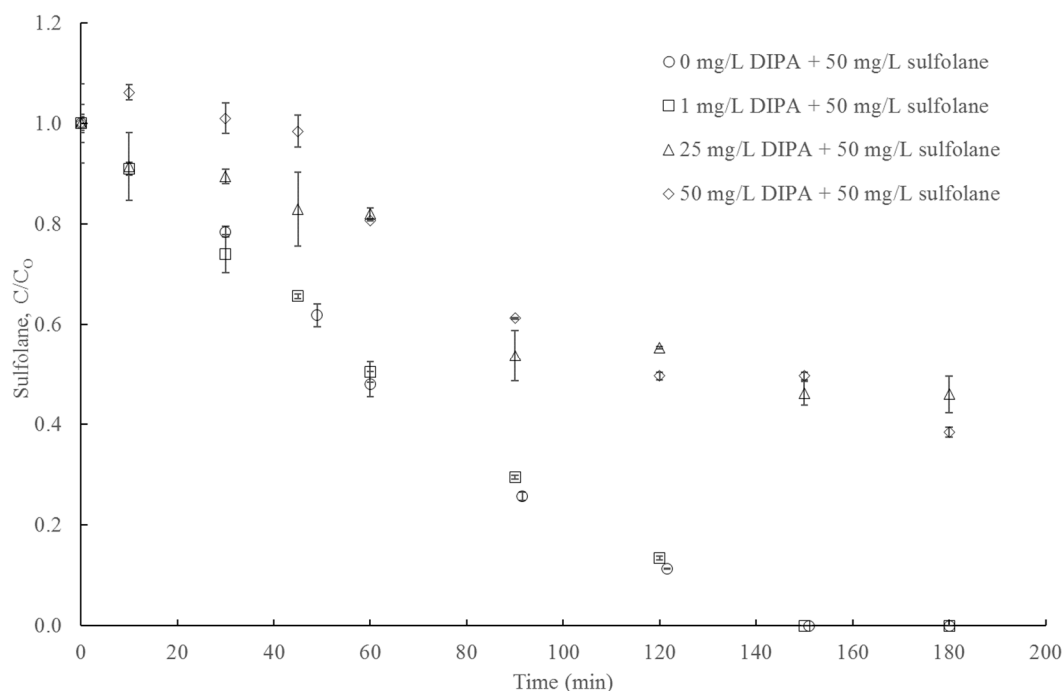

Figure 3. Photocatalytic degradation of sulfolane using 2 g/L of TiO_2 and UVA-LED in milli-Q water, tap water, and groundwater.

Natural organic matter (NOM) and inorganic ions in natural waters may interfere with photocatalytic degradation [50]. Bicarbonate (HCO_3^-) and carbonate ions (CO_3^{2-}) can serve as hydroxyl radical scavengers, which react with $OH^{\cdot}$ to produce $CO_3^{\cdot}$, a weak and highly selective oxidant [51]. This reduces the amount of $OH^{\cdot}$ available for reacting with sulfolane. HCO_3^- can also react with h^+ formed by TiO_2, adsorbing to the TiO_2 surface and forming a negatively charged layer. This can inhibit the interaction between the TiO_2 surface and the target compound [52]. Studies conducted to understand the effect of inorganic ions on photocatalytic degradation of dyes and other model organic compounds found that, similar to HCO_3^- ions, SO_4^{2-} and Cl^- can adsorb onto the TiO_2 surface and trap h^+ and $OH^{\cdot}$ [53]. SO_4^{2-}, Cl^-, and HCO_3^- concentrations are significantly higher in the groundwater and tap water tested, when compared to milli-Q water. It is likely that during the initial 30 min of dark time, inorganic ions coated the TiO_2 surface, resulting in reduced photocatalytic degradation of sulfolane. Studies on cations like Ca^{2+} and Mg^{2+} showed negligible effects on photocatalytic degradation of organic pollutant [54]. This is likely due to their inability to scavenge oxidant species as they already exist at their maximum oxidation state.

Since DIPA and sulfolane are commonly used together in industrial processes, DIPA is often present in sulfolane-contaminated waters [55]. The photocatalytic degradation of samples containing 50 mg/L of sulfolane and varying concentrations of DIPA was studied in this section. The results presented in Figure 4 show that sulfolane degradation was observed in samples with all levels of DIPA concentrations. However, a lag in sulfolane degradation can be observed in the samples containing 25 and 50 mg/L of DIPA. This lag can be explained by the competing effect of DIPA. In this case, the co-contaminant may scavenge photons, absorption sites, and/or photo-induced holes or hydroxyl radicals.

UV-Visible spectroscopy of DIPA showed that no absorption peaks were observed above 300 nm; therefore, photon scavenging by DIPA can be disregarded. Some studies have used TiO_2 photocatalysts to treat aqueous solutions containing DIPA. Mahirah et al. [56] demonstrated that degradation of DIPA by TiO_2 took place mainly by photocatalytic oxidation, and adsorption of DIPA onto the surface of the photocatalyst was minimal in comparison. Since DIPA can be degraded through photocatalysis, it may be using up the hydroxyl radicals and holes produced during photoactivation of TiO_2. In this case, DIPA may be getting preferentially degraded in the mixtures containing 25 mg/L, and greater, of DIPA.

Figure 4. Photocatalytic degradation of sulfolane by TiO_2 (2 g/L) in the presence of varying concentrations of DIPA.

2.4. Recyclability of TiO_2-P25

P25 photocatalyst was used for three consecutive photocatalytic cycles to study the performance and reusability of P25. As shown in Figure 5, degradation of sulfolane was achieved in all three photocatalytic cycles, indicating that the TiO_2 was still active during the final cycle. However, a slight drop in degradation rate suggests that the activity of the photocatalyst decreased in each consecutive cycle. The photocatalyst loading, degradation rate, and removal of sulfolane are shown in Table 2. About 10% and 18% of photocatalyst was lost during the filtering and cleaning process used to recover the P25 after cycles 1 and 2, respectively. Loss of photocatalyst surface may contribute to the decrease in degradation rate. Another factor may be the deactivation of photocatalyst surface by the products of sulfolane mineralization. Abdullah et al. [57] found that sulfate ions can reduce photocatalytic degradation rate by covering photoactive sites on the surface of the TiO_2, deactivating the photocatalyst for degradation of organic molecules. Sulfate ions can be produced as a result of oxidation of sulfolane by hydroxyl radicals [13,14]. As a result, deactivation of photoactive sites by oxidation by-products is a probable cause for the increase in residual sulfolane concentration observed after each consecutive photocatalytic cycle.
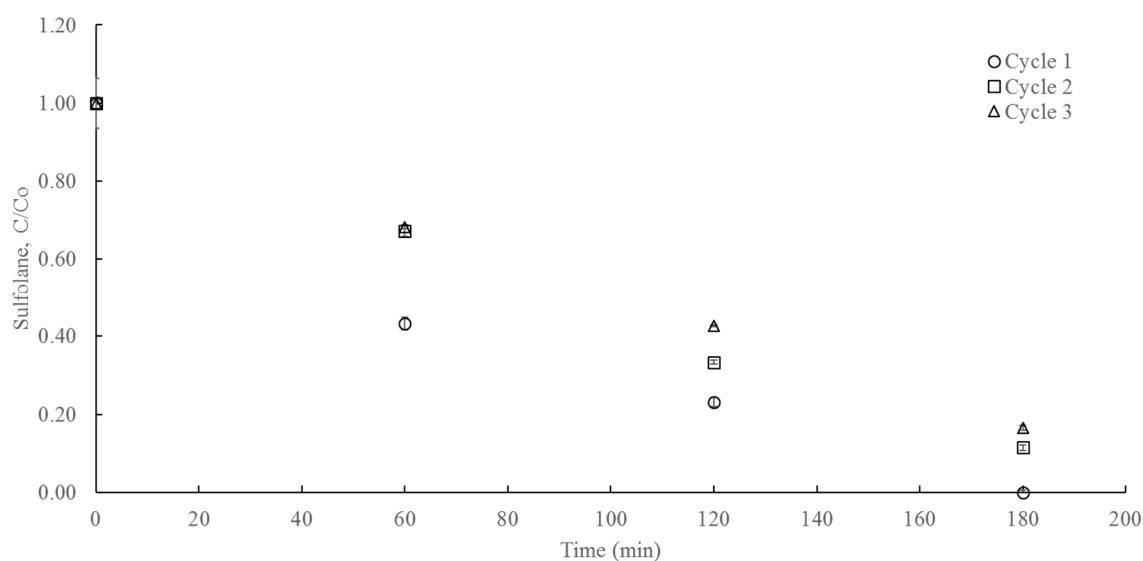
Figure 5. Photocatalytic degradation of sulfolane by TiO_2 in multiple cycles.

Table 2. Sulfolane degradation rate in three photocatalytic cycles.

Cycle	P25 (mg)	Degradation Rate (min^{-1})	P25 Loading (g/L)	Removal after 3 h
Cycle 1	160.4	5.2×10^{-3}	2.005	98%
Cycle 2	143.3	5.0×10^{-3}	1.791	89%
Cycle 3	117.5	4.6×10^{-3}	1.469	85%

3. Materials and Methods

3.1. Chemicals

Sulfolane with 99% purity, ACS grade dichloromethane (DCM), and DIPA with 99% purity were obtained from Sigma Aldrich, Canada (Oakville, ON, Canada). Powdered TiO_2-P25 was procured from Evonik Canada Inc. (Burlington ON, Canada). Graphene oxide suspension was obtained from ACS Chemical Inc. (Point Pleasant, NJ, USA). RGO-P25 composites were synthesized in the lab using the hydrothermal method described by Li et al. [34] and Zhang et al. [58]. Milli-Q water was used in most experiments, except where groundwater and tap water were used. Properties for the tap water and groundwater used in this study are listed in Table 3.

3.2. Photoreactor

An LED photoreactor, originally fabricated by Yu et al. [30], was used for most of the photocatalytic experiments. This cylindrical photoreactor is lined on the inside with 90 UV LEDs (λ_{max} = 365 nm, full-width half-maximum = 12 nm, NSHU551B), arranged in 6 rows of 15 LEDs, and fixed with a fan. Figure 6a shows a vertical cross-section of this LED photoreactor. An LZC-ORG reactor (Luzchem Research Inc., Ottawa, ON, Canada), with the capacity to hold 10 fluorescent lamps, was obtained from Luzchem Research Inc. for the experiments using mercury lamps (Figure 6b). Ten black lamps (LZC-UVA16) centered at 350 nm, and germicidal lamps (LZC-UVC16), at 254 nm, were installed in this reactor for the UVA and UVC mercury lamp experiments, respectively. The number of photons entering the reaction beaker per unit time in both reactors were determined using ferrioxalate actinometry [59]. They were 9.06×10^{16}, 1.74×10^{17}, and 1.85×10^{17} photon/s for the LED photoreactor, the Luzchem reactor equipped with UVA lamps, and the Luzchem reactor equipped with UVC lamps, respectively.

Table 3. Characteristics of groundwater and tap water.

| Parameters	Unit	Groundwater	Tap Water
Total Anion	meq/L	10.6	-
Total Cation	meq/L	11.2	-
Hardness ($CaCO_3$)	mg/L	538	214
Ion Balance	N/A	1.06	-
Dissolved Nitrate (NO_3)	mg/L	0.989	0.08
Nitrate plus Nitrite (N)	mg/L	0.224	-
Dissolved Nitrite (NO_2)	mg/L	<0.033	<0.003
Total Dissolved Solids	mg/L	544	265
Conductivity	uS/cm	975	448
pH	pH	7.67	7.6
Alkalinity (PP as $CaCO_3$)	mg/L	<0.50	-
Alkalinity (Total as $CaCO_3$)	mg/L	445	144
Bicarbonate (HCO_3)	mg/L	542	144
Carbonate (CO_3)	mg/L	<0.50	<20
Hydroxide (OH)	mg/L	<0.50	-
Dissolved Sulphate (SO_4)	mg/L	60.6	74
Dissolved Chloride (Cl)	mg/L	13.6	11
Dissolved Nitrite (N)	mg/L	<0.010	<0.003
Dissolved Nitrate (N)	mg/L	0.224	0.08
Dissolved Calcium (Ca)	mg/L	152	54
Dissolved Iron (Fe)	mg/L	<0.060	<0.010
Dissolved Magnesium (Mg)	mg/L	38.3	17
Dissolved Manganese (Mn)	mg/L	0.0796	<0.0005
Dissolved Potassium (K)	mg/L	2.35	1.1
Dissolved Sodium (Na)	mg/L	9	9

3.3. Experimental Procedure

All experiments were conducted in batch mode in either the LED or Luzchem photoreactors, as shown in Figure 6. Reactions were carried out with 80 mL of solution in either a 100 mL glass beaker (for reactions in UVA-LED) or 150 mL quartz beaker (for UVA and UVC fluorescent mercury lamps). The 50 mg/L solution of sulfolane was prepared using pure sulfolane and the water of interest along with 2 g/L of powdered photocatalyst (either P25 or RGO-P25). A 30 min dark experiment was conducted at the beginning of every experiment to observe the amount of sulfolane adsorbed to the photocatalyst in the absence of light. The solution was continuously stirred throughout the dark and irradiated experiments to homogenize the solution and to ensure adequate distribution of sulfolane and photocatalyst throughout the field of irradiation. Samples were collected at predetermined time intervals, immediately filtered using 0.2 μm polytetrafluoroethylene (PTFE) filters and stored in the dark before extraction and analysis. Additional parameters for each set of experiments can be found in Table 4. It is noted that all experiments were conducted in duplicate, and the average concentration with the error bar indicating the variation between the duplicates were reported in all figures.

3.4. Analytical Methods

Extraction of sulfolane was carried out using 1.5 mL of the water sample and 1.5 mL of DCM in a liquid–liquid extraction. The samples were shaken in a mechanical shaker for 30 min. The DCM phase was then extracted and analyzed. An Agilent 6890 gas chromatograph (GC) (Agilent, Santa Clara, CA, USA), equipped with a flame ionization detector (FID) and an auto sampler, was used to analyze the extracted sulfolane samples in DCM. The Agilent ChemStation software, (Agilent, Santa Clara, CA, USA) was used to carry out data acquisition and calibration. Chromatographic separation was achieved on a fused silica capillary column (ZB 5MSI, Phenomenex, Torrance, CA, USA) upon injection of the DCM samples into the GC. High-purity helium, with a head pressure of 250 kPa, was used as the carrier gas. Sample injection was adjusted to splitless mode with a 1.00 mL

injection volume and the injection port temperature was 165 °C. The initial temperature was set to 90 °C, held constant for 2 min, then ramped up to 175 °C at a rate of 10 °C/min, where it was held constant for 3 min. The FID detector temperature was set to 330 °C.
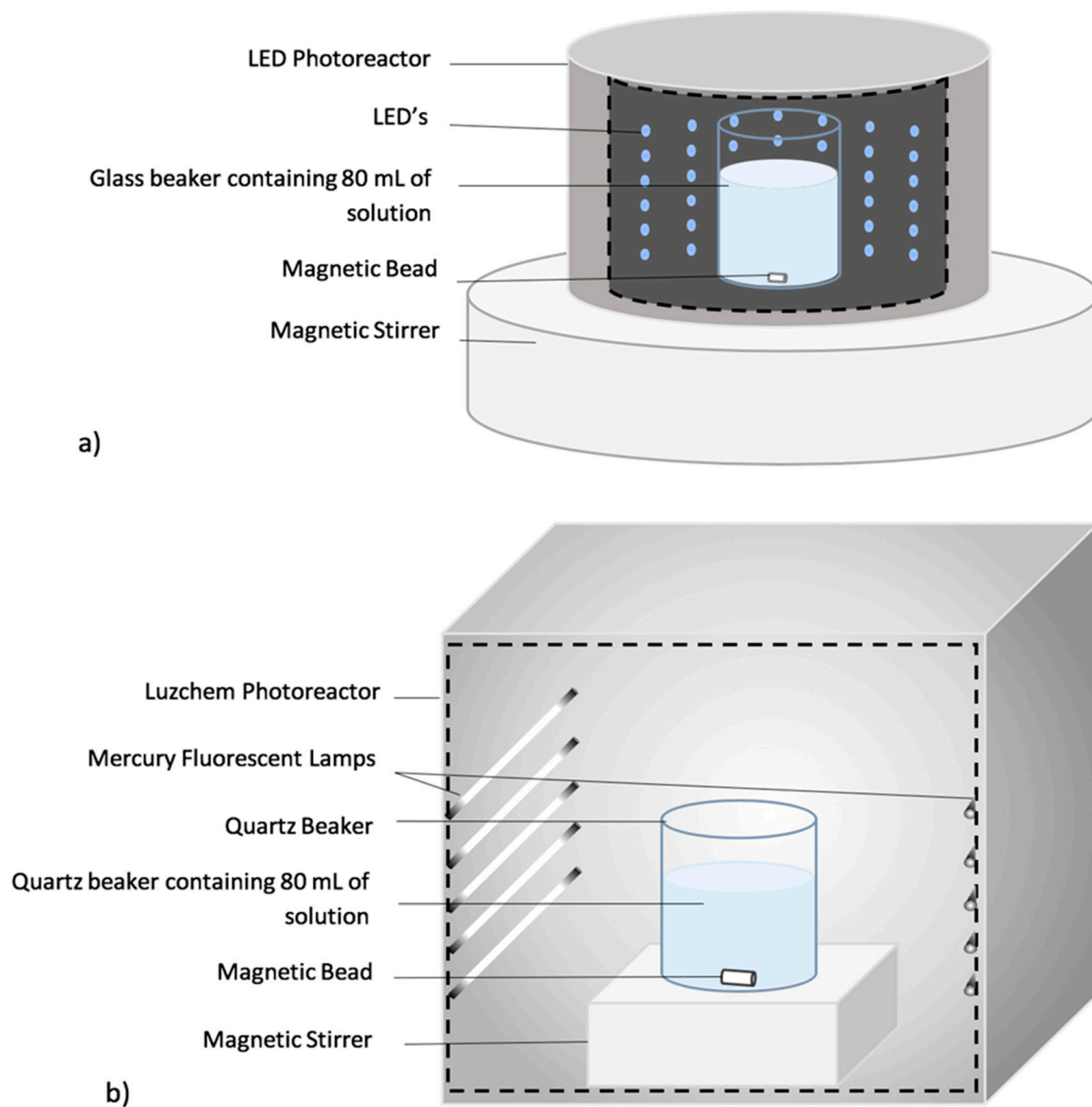
Figure 6. Schematic representation of the experimental setup, where (**a**) depicts the experiments conducted in the UVA-LED photoreactor and (**b**) depicts the experiments conducted in the Luzchem reactor. Each experiment was conducted on 80 mL of a 50 mg/L sulfolane solution with 2 g/L of the photocatalyst of interest. The schematic is not drawn to scale.

Table 4. Details of photocatalytic degradation experiments.

No.	Light Source	Photocatalyst	Photocatalyst Loading (g/L)	Water Matrix	Sulfolane (mg/L)	DIPA (mg/L)	Run
1	UVA-LED	P25	2	Milli-Q	50	0	1
2	UVA-LED	RGO-P25	2	Milli-Q	50	0	1
3	UVA-LED	P25	2	Milli-Q	50	0	1
4	UVA Mercury	P25	2	Milli-Q	50	0	1
5	UVC Mercury	P25	2	Milli-Q	50	0	1
6	UVA-LED	P25	2	Milli-Q	50	0	1
7	UVA-LED	P25	2	Groundwater	50	0	1
8	UVA-LED	P25	2	Tap Water	50	0	1
9	UVA-LED	P25	2	Milli-Q	50	0	1
10	UVA-LED	P25	2	Milli-Q	50	1	1
11	UVA-LED	P25	2	Milli-Q	50	20	1
12	UVA-LED	P25	2	Milli-Q	50	50	1
13	UVA-LED	P25	2	Milli-Q	50	0	1
14	UVA-LED	P25	2	Milli-Q	50	0	2
15	UVA-LED	P25	2	Milli-Q	50	0	3

4. Conclusions

In this paper, a comprehensive study on the photocatalytic degradation of sulfolane in water using UVA-LED was conducted. The results showed that UVA-LED-based photocatalysis is a promising technology to treat sulfolane in aqueous media as it does not require large amounts of chemicals and utilizes less photon energy than mercury lamps. TiO_2 integrated with UVA-LED can degrade more than 99% of sulfolane from water over three hours of irradiation. Extended irradiation can lead to complete mineralization of sulfolane. A recyclability study on TiO_2 showed that it can be used for multiple cycles without significantly losing its photocatalytic activity. Compared to UVA mercury lamps, UVA-LEDs saved 23% of photon energy consumption in achieving one log reduction of sulfolane. TiO_2-RGO composite synthesized through the hydrothermal method did not display enhanced photocatalytic performance for the degradation of sulfolane due to its weak adsorption on TiO_2-RGO composite.

Photocatalytic degradation of sulfolane in groundwater and tap water were observed to be slower than that in ultrapure water due to the high sulfate, chloride, and bicarbonate content in the tap water and groundwater. The sulfolane degradation rate decreased by 43% and 74% in tap water and groundwater respectively, when compared with milli-Q water. The presence of DIPA (>25 mg/L), a co-contaminant frequently detected in the sulfolane-contaminated water, also inhibited photocatalytic degradation of sulfolane.

Author Contributions: Methodology, S.D., L.Y., and G.A.; investigation, S.D. and L.Y.; data curation, S.D. and L.Y.; writing—original draft preparation, S.D. and L.Y.; writing—review and editing, L.Y. and G.A.; supervision, G.A.; project administration, G.A. All authors have read and agreed to the published version of the manuscript.

Data Availability Statement: All data used during the study appear in the published article.

Conflicts of Interest: The authors declare no conflict of interest.

References

1. Tilstam, U. Sulfolane: A Versatile Dipolar Aprotic Solvent. *Org. Process Res. Dev.* **2012**, *16*, 1273–1278. [CrossRef]
2. CCME. *Canadian Environmental Quality Guidelines for Sulfolane: Water and Soil: Scientific Supporting Document*; Canadian Council of Ministers of the Environment: Winnipeg, Man, 2006; ISBN 978-1-896997-59-9.
3. Luther, S.M.; Dudas, M.J.; Fedorak, P.M. Sorption of Sulfolane and Diisopropanolamine by Soils, Clays and Aquifer Materials. *J. Contam. Hydrol.* **1998**, *32*, 159–176. [CrossRef]

4. Stewart, O.; Minnear, L. *Sulfolane Technical Assistance and Evaluation Report Prepared for Alaska Department of Environmental Conservation*; Oasis Environmental: Anchorage, AK, USA, 2010.

5. Gordon, C.J.; Dyer, R.S.; Long, M.D.; Fehlner, K.S. Effect of Sulfolane on Behavioral and Autonomic Thermoregulation in the Rat. *J. Toxicol. Environ. Health* **1985**, *16*, 461–468. [CrossRef]

6. Andersen, M.E.; Jones, R.A.; Mehl, R.G.; Hill, T.A.; Kurlansik, L.; Jenkins, L.J. The Inhalation Toxicity of Sulfolane (Tetrahydrothiophene-1,1-Dioxide). *Toxicol. Appl. Pharmacol.* **1977**, *40*, 463–472. [CrossRef]

7. Shah, S.M.; Wahba, M.; Yu, L.; Achari, G.; Habibi, H.R. Health Impact Assessment of Sulfolane on Embryonic Development of Zebrafish (Danio Rerio). *Toxics* **2019**, *7*, 42. [CrossRef]

8. Kasanke, C.P.; Leigh, M.B. Factors Limiting Sulfolane Biodegradation in Contaminated Subarctic Aquifer Substrate. *PLoS ONE* **2017**, *12*, e0181462. [CrossRef] [PubMed]

9. Greene, E.A.; Gieg, L.M.; Coy, D.L.; Fedorak, P.M. Sulfolane Biodegradation Potential in Aquifer Sediments at Sour Natural Gas Plant Sites. *Water Res.* **1998**, *32*, 3680–3688. [CrossRef]

10. Fedorak, P.M.; Coy, D.L. Biodegradation of Sulfolane in Soil and Groundwater Samplesfrom a Sour Gas Plant Site. *Environ. Technol.* **1996**, *17*, 1093–1102. [CrossRef]

11. McLeod, D.W.; Lin, C.Y.; Ying, W.-C.; Tucker, M.E. Biological Activated Carbon Process for Removing Sulfolane from Groundwater. In Proceedings of the 46th Industrial Waste Conference, West Lafayette, Indiana, 14–16 May 1991; Purdue University: West Lafayette, Indiana, 1991; pp. 99–112.

12. Yu, L.; Mehrabani-Zeinabad, M.; Achari, G.; Langford, C.H. Application of UV Based Advanced Oxidation to Treat Sulfolane in an Aqueous Medium. *Chemosphere* **2016**, *160*, 155–161. [CrossRef]

13. Mehrabani-Zeinabad, M.; Yu, L.; Achari, G.; Langford, C.H. Mineralisation of Sulfolane by UV/O3/H2O2 in a Tubular Reactor. *J. Environ. Eng. Sci.* **2016**, *11*, 44–51. [CrossRef]

14. Izadifard, M.; Achari, G.; Langford, C.H. Degradation of Sulfolane Using Activated Persulfate with UV and UV-Ozone. *Water Res.* **2017**, *125*, 325–331. [CrossRef] [PubMed]

15. Khan, M.F.; Yu, L.; Achari, G.; Tay, J.H. Chemosphere Degradation of Sulfolane in Aqueous Media by Integrating Activated Sludge and Advanced Oxidation Process. *Chemosphere* **2019**, *222*, 1–8. [CrossRef] [PubMed]

16. Crini, G.; Lichtfouse, E. Advantages and Disadvantages of Techniques Used for Wastewater Treatment. *Environ. Chem. Lett.* **2019**, *17*, 145–155. [CrossRef]

17. Nakata, K.; Fujishima, A. TiO$_2$ Photocatalysis: Design and Applications. *J. Photochem. Photobiol. C Photochem. Rev.* **2012**, *13*, 169–189. [CrossRef]

18. Parrino, F.; Bellardita, M.; García-López, E.I.; Marcì, G.; Loddo, V.; Palmisano, L. Heterogeneous Photocatalysis for Selective Formation of High-Value-Added Molecules: Some Chemical and Engineering Aspects. *ACS Catal.* **2018**, *8*, 11191–11225. [CrossRef]

19. Pulgarin, C.; Rinco, A. Comparative Evaluation of Fe 3 + and TiO 2 Photoassisted Processes in Solar Photocatalytic Disinfection of Water. *Appl. Catal. B Environ.* **2006**, *63*, 222–231. [CrossRef]

20. Bakbolat, B.; Daulbayev, C.; Sultanov, F.; Beissenov, R.; Umirzakov, A.; Mereke, A.; Bekbaev, A.; Chuprakov, I. Recent Developments of TiO2-Based Photocatalysis in the Hydrogen Evolution and Photodegradation: A Review. *Nanomaterials* **2020**, *10*, 1790. [CrossRef]

21. Kou, J.; Lu, C.; Wang, J.; Chen, Y.; Xu, Z.; Varma, R.S. Selectivity Enhancement in Heterogeneous Photocatalytic Transformations. *Chem. Rev.* **2017**, *117*, 1445–1514. [CrossRef]

22. Chen, Y.; Xiang, Z.; Wang, D.; Kang, J.; Qi, H. Effective Photocatalytic Degradation and Physical Adsorption of Methylene Blue Using Cellulose/GO/TiO$_2$ hydrogels. *RSC Adv.* **2020**, *10*, 23936–23943. [CrossRef]

23. Kumar, K.Y.; Saini, H.; Pandiarajan, D.; Prashanth, M.K.; Parashuram, L.; Raghu, M.S. Controllable Synthesis of TiO2 Chemically Bonded Graphene for Photocatalytic Hydrogen Evolution and Dye Degradation. *Catal. Today* **2020**, *340*, 170–177. [CrossRef]

24. Lettieri, S.; Gargiulo, V.; Pallotti, D.K.; Vitiello, G.; Maddalena, P.; Alfè, M.; Marotta, R. Evidencing Opposite Charge-Transfer Processes at TiO$_2$/Graphene-Related Materials Interface through Combined EPR, Photoluminescence and Photocatalysis Assessment. *Catal. Today* **2018**, *315*, 19–30. [CrossRef]

25. Ali, M.H.H.; Al-Qahtani, K.M.; El-Sayed, S.M. Enhancing Photodegradation of 2,4,6 Trichlorophenol and Organic Pollutants in Industrial Effluents Using Nanocomposite of TiO2 Doped with Reduced Graphene Oxide. *Egypt. J. Aquat. Res.* **2019**, *45*, 321–328. [CrossRef]

26. Ruidíaz-Martínez, M.; Álvarez, M.A.; López-Ramón, M.V.; Cruz-Quesada, G.; Rivera-Utrilla, J.; Sánchez-Polo, M. Hydrothermal Synthesis of RGO-TiO2 Composites as High-Performance UV Photocatalysts for Ethylparaben Degradation. *Catalysts* **2020**, *10*, 520. [CrossRef]

27. Ghosh, J.P.; Sui, R.; Langford, C.H.; Achari, G.; Berlinguette, C.P. A Comparison of Several Nanoscale Photocatalysts in the Degradation of a Common Pollutant Using LEDs and Conventional UV Light. *Water Res.* **2009**, *43*, 4499–4506. [CrossRef]

28. Shie, J.L.; Lee, C.H.; Chiou, C.S.; Chang, C.T.; Chang, C.C.; Chang, C.Y. Photodegradation Kinetics of Formaldehyde Using Light Sources of UVA, UVC and UVLED in the Presence of Composed Silver Titanium Oxide Photocatalyst. *J. Hazard. Mater.* **2008**, *155*, 164–172. [CrossRef]

29. Autin, O.; Romelot, C.; Rust, L.; Hart, J.; Jarvis, P.; MacAdam, J.; Parsons, S.A.; Jefferson, B. Evaluation of a UV-Light Emitting Diodes Unit for the Removal of Micropollutants in Water for Low Energy Advanced Oxidation Processes. *Chemosphere* **2013**, *92*, 745–751. [CrossRef]

30. Yu, L.; Achari, G.; Langford, C.H. LED-Based Photocatalytic Treatment of Pesticides and Chlorophenols. *J. Environ. Eng.* **2013**, *139*, 1146–1151. [CrossRef]

31. Ran, Z.; Fang, Y.; Sun, J.; Ma, C.; Li, S. Photocatalytic Oxidative Degradation of Carbamazepine by TiO_2 Irradiated by UV Light Emitting Diode. *Catalysts* **2020**, *10*, 540. [CrossRef]

32. Eskandarian, M.R.; Choi, H.; Fazli, M.; Rasoulifard, M.H. Effect of UV-LED Wavelengths on Direct Photolytic and TiO_2 Photocatalytic Degradation of Emerging Contaminants in Water. *Chem. Eng. J.* **2016**, *300*, 414–422. [CrossRef]

33. Dharwadkar, S.; Yu, L.; Achari, G. Enhancement of LED Based Photocatalytic Degradation of Sulfolane by Integration with Oxidants and Nanomaterials. *Chemosphere* **2021**, *263*, 128124. [CrossRef]

34. Li, J.; Zhou, S.L.; Hong, G.B.; Chang, C.T. Hydrothermal Preparation of P25–Graphene Composite with Enhanced Adsorption and Photocatalytic Degradation of Dyes. *Chem. Eng. J.* **2013**, *219*, 486–491. [CrossRef]

35. Yu, F.; Bai, X.; Yang, C.; Xu, L.; Ma, J. Reduced Graphene Oxide–P25 Nanocomposites as Efficient Photocatalysts for Degradation of Bisphenol A in Water. *Catalysts* **2019**, *9*, 607. [CrossRef]

36. Zhang, Y.; Tang, Z.; Fu, X.; Xu, Y. TiO_2-Graphene Nanocomposites for Gas-Phase Photocatalytic Degradation of Volatile Aromatic Pollutant: Is TiO_2-Graphene Truly Different From. *ACS Nano* **2010**, *4*, 1–7. [CrossRef]

37. Pan, X.; Zhao, Y.; Liu, S.; Korzeniewski, C.L.; Wang, S.; Fan, Z. Comparing Graphene-TiO_2 Nanowire and Graphene-TiO_2 Nanoparticle Composite Photocatalysts. *ACS Appl. Mater. Interfaces* **2012**, *4*, 3944–3950. [CrossRef]

38. Perera, S.D.; Mariano, R.G.; Vu, K.; Nour, N.; Seitz, O.; Chabal, Y.; Balkus, K.J. Hydrothermal Synthesis of Graphene-TiO_2 Nanotube Composites with Enhanced Photocatalytic Activity. *ACS Catal.* **2012**, *2*, 949–956. [CrossRef]

39. Langford, C.; Izadifard, M.; Radwan, E.; Achari, G. Some Observations on the Development of Superior Photocatalytic Systems for Application to Water Purification by the "Adsorb and Shuttle" or the Interphase Charge Transfer Mechanisms. *Molecules* **2014**, *19*, 19557–19572. [CrossRef]

40. Haldorai, Y.; Rengaraj, A.; Hwan, C.H.; Suk, Y.S.; Han, Y.-K. Fabrication of Nano TiO_2 @ Graphene Composite: Reusable Photocatalyst for Hydrogen Production, Degradation of Organic and Inorganic Pollutants. *Synth. Met.* **2014**, *198*, 10–18. [CrossRef]

41. López, R.; Gómez, R. Band-Gap Energy Estimation from Diffuse Reflectance Measurements on Sol-Gel and Commercial TiO 2: A Comparative Study. *J. Sol-Gel Sci. Technol.* **2012**, *61*, 1–7. [CrossRef]

42. Nagaveni, K.; Hegde, M.S.; Ravishankar, N.; Subbanna, G.N.; Madras, G. Synthesis and Structure of Nanocrystalline TiO2 with Lower Band Gap Showing High Photocatalytic Activity. *Langmuir* **2004**, *20*, 2900–2907. [CrossRef] [PubMed]

43. Zhang, Y.; Pan, C. TiO_2/Graphene Composite from Thermal Reaction of Graphene Oxide and Its Photocatalytic Activity in Visible Light. *J. Mater. Sci.* **2011**, *46*, 2622–2626. [CrossRef]

44. Posa, V.R.; Annavaram, V.; Somala, A.R. Fabrication of Graphene-TiO_2 Nanocomposite with Improved Photocatalytic Degradation for Acid Orange 7 Dye under Solar Light Irradiation. *Bull. Mater. Sci.* **2016**, *39*, 759–767. [CrossRef]

45. Yang, M.-Q.; Nan, Z.; Pagliaro, M.; Xu, Y. Artificial Photosynthesis over Graphene–Semiconductor Composites. Are We Getting Better? *Chem. Soc. Rev.* **2014**, *43*, 8240–8254. [CrossRef] [PubMed]

46. Kamat, P. V Graphene-Based Nanoassemblies for Energy Conversion. *J. Phys. Chem. Lett* **2011**, *2*, 242–251. [CrossRef]

47. Zhang, Y.; Tang, Z.-R.; Fu, X.; Xu, Y.J. Engineering the Unique 2D Mat of Graphene to Achieve Graphene-TiO_2 Nanocomposite for Photocatalytic Selective Transformation: What Advantage Does Graphene Have over Its Forebear Carbon Nanotube? *ACS Nano* **2011**, *5*, 7426–7435. [CrossRef] [PubMed]

48. Akhavan, O.; Abdolahad, M.; Esfandiar, A.; Mohatashamifar, M. Photodegradation of Graphene Oxide Sheets by TiO2 Nanoparticles after a Photocatalytic Reduction. *J. Phys. Chem. C* **2010**, *114*, 12955–12959. [CrossRef]

49. Bhatkhande, D.S.; Kamble, S.P.; Sawant, S.B.; Pangarkar, V.G. Photocatalytic and Photochemical Degradation of Nitrobenzene Using Artificial Ultraviolet Light. *Chem. Eng. J.* **2004**, *102*, 283–290. [CrossRef]

50. Hu, L.; Flanders, P.M.; Miller, P.L.; Strathmann, T.J. Oxidation of Sulfamethoxazole and Related Antimicrobial Agents by TiO2 Photocatalysis. *Water Res.* **2007**, *41*, 2612–2626. [CrossRef]

51. Haarstrick, A.; Kut, O.M.; Heinzle, E. TiO_2-Assisted Degradation of Environmentally Relevant Organic Compounds in Wastewater Using a Novel Fluidized Bed Photoreactor. *Environ. Sci. Technol.* **1996**, *30*, 817–824. [CrossRef]

52. Rincón, A.G.; Pulgarin, C. Effect of PH, Inorganic Ions, Organic Matter and H2O2on E. Coli K12 Photocatalytic Inactivation by TiO2: Implications in Solar Water Disinfection. *Appl. Catal. B Environ.* **2004**, *51*, 283–302. [CrossRef]

53. Habibi, M.H.; Hassanzadeh, A.; Mahdavi, S. The Effect of Operational Parameters on the Photocatalytic Degradation of Three Textile Azo Dyes in Aqueous TiO_2 Suspensions. *J. Photochem. Photobiol. A Chem.* **2005**, *172*, 89–96. [CrossRef]

54. Chong, M.N.; Jin, B.; Chow, C.W.K.; Saint, C. Recent Developments in Photocatalytic Water Treatment Technology: A Review. *Water Res.* **2010**, *44*, 2997–3027. [CrossRef] [PubMed]

55. Greene, E.A.; Coy, D.L.; Fedorak, P.M. Laboratory Evaluations of Factors Affecting Biodegradation of Sulfolane and Diisopropanolamine. *Bioremediation J.* **1999**, *3*, 299–313. [CrossRef]

56. Ramli, R.M.; Kait, C.F.; Omar, A.A. Remediation of DIPA Contaminated Wastewater Using Visible Light Active Bimetallic Cu-Fe/TiO_2 Photocatalyst. *Procedia Eng.* **2016**, *148*, 508–515. [CrossRef]

57. Abdullah, M.; Low, G.K.C.; Matthews, R.W. Effects of Common Inorganic Anions on Rates of Photocatalytic Oxidation of Organic Carbon over Illuminated Titanium Dioxide. *J. Phys. Chem.* **1990**, *94*, 6820–6825. [CrossRef]

58. Zhang, H.; Lv, X.; Li, Y.; Wang, Y.; Li, J. P25-Graphene Composite as a High Performance Photocatalyst. *ACS Nano* **2010**, *4*, 380–386. [CrossRef] [PubMed]

59. Hatchard, C.G.; Parker, C.A. A New Sensitive Chemical Actinometer—II. Potassium Ferrioxalate as a Standard Chemical Actinometer. *Proc. R. Soc. Lond. Ser. A Math. Phys. Sci.* **1956**, *235*, 518–536. [CrossRef]